

Quantum mechanics and hidden variables: A test of Bell's inequality by the measurement of the spin correlation in low-energy proton-proton scattering

M. Laméhi-Rachti and W. Mittig*

Département de Physique Nucléaire, CEN Saclay, BP2, 91190 Gif-sur-Yvette, France

(Received 11 August 1975; revised manuscript received 26 July 1976)

The inequality of Bell has been tested by the measurement of the spin correlation in proton-proton scattering. Measurements were made at $E_p = 13.2$ and 13.7 MeV using carbon analyzers of 18.6 and 29 mg/cm², respectively, accumulating a total of 10^4 coincidences. The experimental analyzing power, geometric correlation coefficients, and energy spectra are compared to the result of a Monte Carlo simulation of the apparatus. The results are in good agreement with quantum mechanics and in disagreement with the inequality of Bell if the same additional assumptions are made. The conditions for comparing the results of the experiments to the inequality of Bell are discussed.

I. INTRODUCTION

Since the beginning of quantum mechanics (QM) a number of physicists who contributed the most to the development of this theory had serious doubts about its logical foundations. Most of the problems were illustrated by a number of paradoxes, such as those of Einstein, Podolsky, and Rosen¹ and Schrödinger (namely, the cat paradox).² These discussions never died down and even today there is no theory of measurement which satisfies everybody.

One attempt to overcome these difficulties was to suppose that there are some supplementary variables outside the scope of QM ("hidden variables") which determine the result of the individual measurement. A theorem derived by J. von Neumann was taken for a long time as proof that such interpretations are impossible. But Bohm³ in 1952 developed a model of the hidden-variables theory which was in complete agreement with the predictions of QM, and Bell⁴ showed in 1965 why the theorem of von Neumann was not valid as applied to physical systems. Bell showed, too, that all hidden-variables models which give complete agreement with QM must have an undesirable feature. They do not obey the principle of locality as stated by Einstein⁵: "If S_1 and S_2 are two systems that have interacted in the past but are now arbitrarily distant, the real, factual situation of system S_1 does not depend on what is done with system S_2 , which is spatially separated from the former."

Developments⁶⁻⁸ of the argumentation of Bell led for the first time in a more than 30-year-old discussion to the possibility of a critical experimental test which could distinguish among the different interpretations. The consequences of such experimental verifications have more profound implications than just eliminating special models which

interpret the measuring process. They will test the validity of a general conception of the foundations of microphysics: the principle of locality or, as written more precisely in Ref. 7, the validity of objective local theories.

II. BELL'S INEQUALITY

The first derivation of the inequality, which later led to an experimental test, was given by Bell.⁴ It has been generalized by Clauser *et al.*^{6,7} In the meantime various ways of demonstration have been derived and can be found in Ref. 9 together with a description of the actual state of hidden-variables theories. We will follow here a demonstration given by Bell.⁸

To be definite we take the example of two spin- $\frac{1}{2}$ particles which have been coupled in the past in a singlet state and which are now widely separated. The principle of locality as formulated by Einstein means that each of these particles has some properties, which we will denote by λ (λ can be a whole set of variables) which do *not* depend on what is happening to the other particle. The result of the measurement is determined by these properties λ . We denote by A , B the result of the measurement in the direction \vec{a} and \vec{b} of the sign of the spin of the two particles respectively. For a realistic apparatus and/or if the dependence on λ is not strictly deterministic, but only stochastic, one will have

$$|A(\lambda, \vec{a})| \leq 1 \text{ and } |B(\lambda, \vec{b})| \leq 1.$$

The correlation function $P(\vec{a}, \vec{b})$ is defined to be the mean value of the product AB and thus

$$P(\vec{a}, \vec{b}) = \int A(\lambda, \vec{a})B(\lambda, \vec{b})\rho(\lambda)d\lambda,$$

where $\rho(\lambda)$ denotes the frequency of the properties λ with the normalization condition $\int \rho(\lambda)d\lambda = 1$.

Thus,

$$\begin{aligned}
|P(\vec{a}, \vec{b}) - P(\vec{a}, \vec{b}')| &= \left| \int A(\lambda, \vec{a})B(\lambda, \vec{b})\rho(\lambda)d\lambda - \int A(\lambda, \vec{a})B(\lambda, \vec{b}')\rho(\lambda)d\lambda \pm \int A(\lambda, \vec{a})B(\lambda, \vec{b})A(\lambda, \vec{a}')B(\lambda, \vec{b}')\rho(\lambda)d\lambda \right. \\
&\quad \left. \mp \int A(\lambda, \vec{a})B(\lambda, \vec{b}')A(\lambda, \vec{a}')B(\lambda, \vec{b})\rho(\lambda)d\lambda \right| \\
&= \left| \int A(\lambda, \vec{a})B(\lambda, \vec{b})[1 \pm A(\lambda, \vec{a}')B(\lambda, \vec{b}')] \rho(\lambda)d\lambda - \int A(\lambda, \vec{a})B(\lambda, \vec{b}') [1 \pm A(\lambda, \vec{a}')B(\lambda, \vec{b})] \rho(\lambda)d\lambda \right| \\
&\leq \int |A(\lambda, \vec{a})B(\lambda, \vec{b})| [1 \pm A(\lambda, \vec{a}')B(\lambda, \vec{b}')] \rho(\lambda)d\lambda + \int |A(\lambda, \vec{a})B(\lambda, \vec{b}')| [1 \pm A(\lambda, \vec{a}')B(\lambda, \vec{b})] \rho(\lambda)d\lambda \\
&\leq 2[P(\vec{a}', \vec{b}') + P(\vec{a}', \vec{b})] \quad \text{using } |AB| \leq 1.
\end{aligned}$$

For coplanar vectors \vec{a} , \vec{a}' , \vec{b} , \vec{b}' only the angle between these vectors is important, and one can write

$$|P(\theta) - P(\theta + \gamma)| + |P(\theta + \gamma + \phi) + P(\theta + \phi)| \leq 2.$$

QM predicts for this correlation function^{4, 17, 18}

$$\begin{aligned}
P(\vec{a}, \vec{b})_{\text{QM}} &= \langle \vec{\sigma}_1 \cdot \vec{a} \vec{\sigma}_2 \cdot \vec{b} \rangle \\
&= -\cos(\vec{a}, \vec{b}) \\
&= -\cos\theta.
\end{aligned}$$

Putting in special values for the angles θ, γ, ϕ and using the invariance of P by reflection and rotation one gets the upper limits for the absolute value of $P(\theta)$ as compared to predictions of QM in Table I. As can be seen, there is a definite contradiction between the values predicted by QM and the upper limit as implied by the inequality of Bell.

III. DESCRIPTION OF A "PERFECT" EXPERIMENTAL SETUP AND DISCUSSION OF REALIZED EXPERIMENTS

The inequality of Bell can be tested by special experimental devices. We will first describe an example of an ideal experiment and then discuss how the actually performed experiments differ from such an ideal arrangement.

We will take as an example Bohm's¹⁰ version of the Einstein-Podolsky-Rosen paradox. Consider (Fig. 1) a source which prepares two particles of spin $J = \frac{1}{2}$ in an intermediate state $J = 0$. This state disintegrates by emitting the two particles with a velocity v in opposite directions. The two possible states, $+$ and $-$, of the direction of spin are split up for example by Stern-Gerlach magnets and the particles are detected by the detectors d . The vectors \vec{a} and \vec{b} denote the orientations of the magnets. Then we define N_0 as the number of pairs of particles which enter the analyzers in coincidence (preparation of a beam of coincident particles) which would be measured in the case of charged particles of sufficiently high energy for example by the use of thin ΔE counters as entrance collimators of the analyzers without depolarization of the particles. As in Ref. 7 we define $p_1^+(\vec{a}, \lambda)$ as the probability of having a count

in the counter d_1^+ , and in the same way for the other counters. For sufficiently large number N_0 we have

$$p_1^+(\vec{a}) = \frac{N_1^+}{N_0} = \int P_1^+(\vec{a}, \lambda) \rho(\lambda) d\lambda,$$

and clearly $p_1^+(\vec{a}, \lambda) \leq 1$ and $-1 \leq p_1^-(\vec{a}, \lambda) - p_1^+(\vec{a}, \lambda) \leq 1$. For objective local theories one gets

$$\frac{N_{++}}{N_0} = \int p_1^+(\vec{a}, \lambda) p_2^+(\vec{b}, \lambda) \rho(\lambda) d\lambda,$$

where N_{++} are coincidences between the counters d_1^+ and d_2^+ .

Defining the measured correlation function as

$$P'_{\text{meas}}(\vec{a}, \vec{b}) = \frac{N_{++} + N_{--} - N_{+-} - N_{-+}}{N_0}$$

and using the above relation for N_{++} and an analogous relation for N_{+-} and so on we get

$$\begin{aligned}
P'_{\text{meas}}(\vec{a}, \vec{b}) &= \int [p_1^+(\vec{a}, \lambda) - p_1^-(\vec{a}, \lambda)] [p_2^+(\vec{b}, \lambda) - p_2^-(\vec{b}, \lambda)] \\
&\quad \times \rho(\lambda) d\lambda.
\end{aligned}$$

Setting

$$p_1^+(\vec{a}, \lambda) - p_1^-(\vec{a}, \lambda) = A(\vec{a}, \lambda)$$

and

$$p_2^+(\vec{b}, \lambda) - p_2^-(\vec{b}, \lambda) = B(\vec{b}, \lambda),$$

we see that this is equivalent to the function $P(\vec{a}, \vec{b})$ defined earlier and thus must obey the same inequality, if objective local theories are valid.

Quantum mechanics predicts for this correlation

TABLE I. Comparison of predictions of QM for $|P(\phi)|$ with the upper limit given by the inequality of Bell.

ϕ	QM	Upper limit of Bell's inequality
0°	1	≤ 1
30°	$\frac{3}{2}$	$\leq \frac{2}{3}$
45°	$1/\sqrt{2}$	$\leq \frac{1}{2}$
60°	$\frac{1}{2}$	$[2 - P(0^\circ)]/3$
90°	0	0

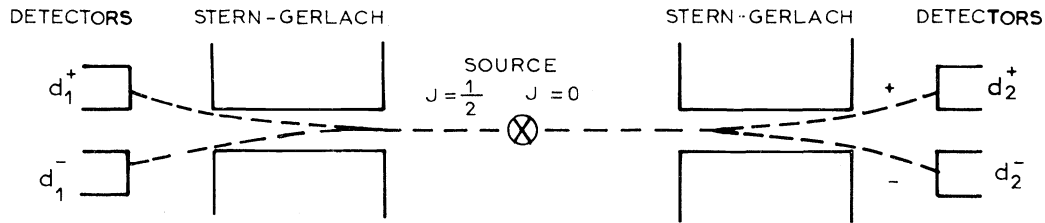


FIG. 1. Schematic experimental setup for the test of the inequality of Bell.

function

$$P'_{\text{meas}}(\vec{a}, \vec{b}) = P_1 P_2 T_1 T_2 \cos(\vec{a}, \vec{b}),$$

where $P_{1,2}$ and $T_{1,2}$ are the analyzing power and transmission of the analyzers. Therefore in order to get a contradiction with the inequality an ideal apparatus should have the property

(a) $|P_1 P_2 T_1 T_2| > 1/\sqrt{2}$, which is a very stringent condition, and supposes yet that one has measured the number of particles which enter the analyzer in coincidence. Apart from this, the ideal apparatus should have the following properties:

(b) The lifetime τ of the intermediate state should be short and the source should be pulsed (or by some other information—coincidence—one should know when the particles enter the analyzers) with a resolution t_r and the restrictions

$$\tau v \ll D \text{ and } t_r v \ll D,$$

where v is the velocity of the particles and D is the dimension of the apparatus. This ensures that one knows at each moment with a good precision where to find the particles in the apparatus.

(c) The time t_v between the moment when the particles enter the analyzer and the detection should satisfy the relation

$$t_v c < d,$$

where c is the speed of light and d is the distance between the analyzers. Thus the theory of relativity excludes the coupling of the particles after or during the measurement process.

(d) The orientation \vec{a}, \vec{b} of the two analyzers should be changed in an arbitrary way during the time of flight of the particles, satisfying the relation

$$(t_{\text{ch}} - t_{\text{det}})c < d,$$

where t_{ch} denotes the time of the change of orientation and t_{det} denotes the time of detection of the particles. Thus one analyzer cannot “know,” with a speed of exchange of information $\leq c$, what the other one is doing.

If all these conditions are satisfied the above-defined correlation can directly be compared to the inequality of Bell without extra assumptions. To

see what can happen if there are deviations from the above-described ideal setup let us consider as an example the case where the detection probability is low, $P_{\text{det}} \ll 100\%$. It is possible to imagine that for a perfect apparatus with $P_{\text{det}} = 100\%$, one would measure a correlation function which agrees with the inequality of Bell. When the detection probability becomes low the properties of the particles, which determine the result of the spin measurement, determine at the same time the probability of joint detection, doing so in such a way that agreement of the counting rates with QM is reestablished. This means that the properties of the particles which determine the result of the spin measurement would determine in a *correlated* way other properties (in this example to be detected or not). One can imagine that for one special experiment there is such a correlation of properties. But it seems difficult to imagine that in very different experimental setups different properties will always be correlated in just such a way to reestablish agreement with QM. This shows that it is necessary to test the inequality of Bell in very different experimental conditions. If the spacelike separation of the particles and of the different parts of the measuring device is not realized, one can imagine some hypothetical coupling or exchange of information. This would mean that the result of the measurement on one particle could depend on what is done with the other particle and agreement with QM could be obtained.

The first experiment done specifically to verify the inequality of Bell was the measurement of the correlation of polarization of positronium annihilation γ rays by Kasday.¹¹ Agreement with QM was obtained. Somewhat later the correlation of polarization of photons of an atomic cascade was studied by Freedman and Clauser,¹² and again agreement with QM was obtained. The experiment with atomic photons has the advantage that in atomic physics one can build polarization analyzers of nearly 100% transmission and analyzing power, which is not the case for the experiment with annihilation γ rays. Some of this advantage is lost by the low probability of response of photomultipliers used to detect the photons ($\sim 10\%$) and

the fact that the second photon is not emitted in a well-defined direction with respect to the first one, but into the whole space. The photon experiment is related to a three-body phenomenon, involving the two photons and the atom which emits the photons. Thus, as in the other experiment, only a very small number of the photons detected in one analyzer is in coincidence with the photons detected in the other analyzer. In the atomic photon experiment the additional assumption necessary concerns the response probability of the photomultiplier ("no enhancement assumption"⁷), whereas in the annihilation γ experiment it concerns the scattering process in the first scatterer.

Both types of experiments used photons. Photons cannot be localized by a Lorentz transformation. One can attribute to photons a length, the coherence length $l = c\tau$, where c is the speed of light and τ is the mean lifetime of the state which produced the photon. For experiments with annihilation γ rays this length is ~ 17 cm and ~ 300 cm for the atomic cascade case. These dimensions are comparable to or bigger than the dimension of the apparatus used and therefore it is not clear that the condition of localization is respected. This is why it had been suggested¹³ that we use particles with a mass at rest different from zero.

We developed an experimental device to measure the spin correlation of protons after scattering in a singlet state, and this will be described in some detail below. Since the beginning of the development of this device the experimental situation for the photons became more confused. The experiment with annihilation γ rays was repeated by Faraci *et al.*¹⁴ and results in contradiction with QM and in agreement with Bell's inequality were obtained. For another atomic cascade Holt and Pipkin¹⁵ found a result which is also in contradiction with QM and in agreement with Bell's inequality. These experiments will be repeated in other laboratories, and so we can hope that in the not-too-distant future the experimental situation for the photon experiments will be clarified.²⁸

IV. MEASUREMENT OF THE SPIN CORRELATION IN LOW-ENERGY PROTON-PROTON SCATTERING

A. The experimental setup

In Fig. 2 the schematic experimental device is shown. A beam of protons, delivered by the Saclay tandem accelerator, hits a target containing hydrogen. After scattering, the two protons enter in kinematical coincidence into the analyzers at $\theta_{lab} = 45^\circ$ ($\theta_{c.m.} = 90^\circ$). In the analyzers the protons are scattered by a carbon foil and the coincidences between the detectors of one analyzer with the detectors of the other are counted. The detectors of one analyzer are in the reaction plane, and the

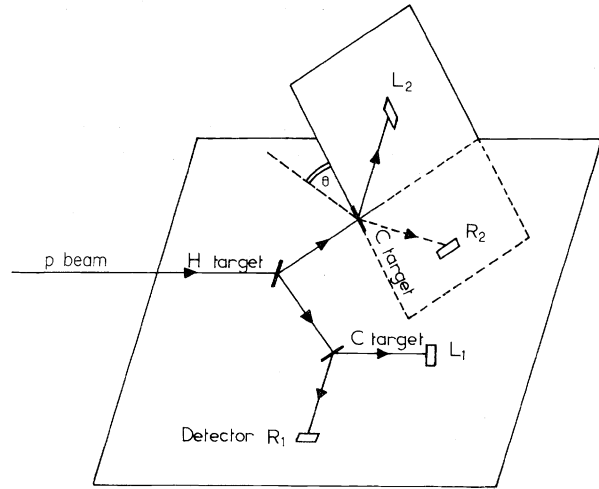


FIG. 2. Schematic experimental setup for the measurement of the spin correlation in proton-proton scattering.

detectors of the other are rotated by an angle θ around the axis defined by the protons entering in the analyzer.

We define the measured correlation function

$$P_{\text{meas}}(a, b) = \frac{N_{LL} + N_{RR} - N_{RL} - N_{LR}}{N_{LL} + N_{RR} + N_{RL} + N_{LR}},$$

where N_{LL} are the coincidences between left counters L_1 and L_2 , and so on.

It is not possible to compare this correlation function directly with the inequality of Bell. Some extra assumptions are necessary because our apparatus does not fulfill the conditions for a perfect apparatus. The following assumptions are necessary:

H1: It is possible to construct a perfect apparatus. As in the annihilation γ case, there is no experimental method known which could give nearly 100% analyzing power and transmission, even extrapolating present techniques. A Stern-Gerlach apparatus is not suited for charged particles as can be shown by uncertainty relations.¹⁶ Nonetheless, there does not seem to exist *a priori* an obstacle to constructing such a perfect apparatus.

H2: Our device does not fulfill the conditions of spacelike separation discussed in the preceding section. We assume that this does not affect the result of the measurement. In the experiment the coherence length can be estimated from the lifetime of the intermediate state formed in p - p scattering. Because there are no sharp resonances this lifetime is of the order of $\tau \approx 10^{-22}$ sec, resulting in a coherence length of $\lambda \approx 4 \times 10^{-13}$ cm. This is very small compared to the dimension of

the apparatus (5 cm), in distinction with the photon experiments where the coherence length and the dimension of the apparatus are of the same order of magnitude. We tried to minimize the distance between the detectors and the carbon foil, in order to prevent a hypothetical coupling between the particles after the second scattering. In our device the time of flight $t_v = 0.3$ nsec, whereas $d/c = 0.2$ nsec. This means that we were quite near the condition (c) in Sec. III, but we did not yet fulfill it.

The analyzing power of our measuring device is ~ 0.7 which is very similar to the one obtained in the annihilation γ experiments and, as in the case of annihilation γ 's the transmission of the analyzers is very low. Therefore the product $P_1 P_2 T_1 T_2$ does not fulfill the conditions of a perfect device. Examples for which it is not possible to compare with the inequality without additional assumptions have been given.^{7, 8, 11} Consider a pair of particles which enter the analyzers in coincidence. Suppose that a perfect device would give the results $p_{1L}^{id}(\vec{a}, \lambda)$, $p_{1R}^{id}(\vec{a}, \lambda)$, etc. for the probability of having a count in the detectors d_{1L} , d_{1R} , etc. It makes sense to consider such a device because of assumption H1. We now make the following assumption:

H3: The analyzing power and the transmission of the measuring apparatus can be considered as intrinsic constants of the apparatus. This means that the parameters λ which determine the result of the spin measurement do not determine in a correlated way the value of the analyzing power and/or transmission of the analyzers. A similar assumption is necessary in the atomic photon experiment concerning the response probability of the photomultipliers.

Then one can write

$$\begin{aligned} p_{1L}(\vec{a}, \lambda) + p_{1R}(\vec{a}, \lambda) &= T_1 [p_{1L}^{id}(\vec{a}, \lambda) + p_{1R}^{id}(\vec{a}, \lambda)] \\ &= T_1, \\ p_{1L}(\vec{a}, \lambda) - p_{1R}(\vec{a}, \lambda) &= T_1 P_1 [p_{1L}^{id}(\vec{a}, \lambda) - p_{1R}^{id}(\vec{a}, \lambda)] \\ &= T_1 P_1 A(\vec{a}, \lambda), \end{aligned}$$

where $p_{1L}(\vec{a}, \lambda)$ is the probability of having a count in the left counter of the analyzer¹ and so on, and P_1 and T_1 are the mean analyzing power and transmission. Analogous equations hold for the apparatus 2.

Then for N_0 particles which enter the analyzers in coincidence, one has

$$\begin{aligned} N_0(p_{1L} - p_{1R})(p_{2L} - p_{2R}) &= N_0 P_1 P_2 T_1 T_2 \\ &\quad \times \int A(\vec{a}, \lambda) B(\vec{b}, \lambda) \rho(\lambda) d\lambda \\ &= N_{LL} + N_{RR} - N_{LR} - N_{RL}, \\ N_0(p_{1L} + p_{1R})(p_{2L} + p_{2R}) &= N_0 T_1 T_2 \\ &= N_{LL} + N_{RR} + N_{LR} + N_{RL}. \end{aligned}$$

Using these relations one has

$$\begin{aligned} P_{\text{meas}}(\vec{a}, \vec{b}) &= \frac{N_{LL} + N_{RR} - N_{LR} - N_{RL}}{N_{LL} + N_{RR} + N_{LR} + N_{RL}} \\ &= P_1 P_2 \int A(\vec{a}, \lambda) B(\vec{b}, \lambda) \rho(\lambda) d\lambda. \end{aligned}$$

The transmission coefficients for left-right scattering of the analyzers depend slightly on the angle ψ of the first scattering. Replacing N_0 by $dN_0/d\psi$ and introducing the dependence of the transmission coefficient on ψ , one finds after some arithmetic and integration between ψ_{\min} and ψ_{\max} a correction to the preceding formula; and the final result is, to first order in the correction term,

$$P_{\text{meas}}(\vec{a}, \vec{b}) = P_1 P_2 \int A(\vec{a}, \lambda) B(\vec{b}, \lambda) \rho(\lambda) d\lambda + C_g \left\{ 1 - \left[P_1 P_2 \int A(\vec{a}, \lambda) B(\vec{b}, \lambda) \rho(\lambda) d\lambda \right]^2 \right\} \cos(\vec{a}, \vec{b}),$$

where

$$C_g = \frac{\int (T_{1L} T_{2L} + T_{1R} T_{2R} - T_{1L} T_{2R} - T_{1R} T_{2L}) d\psi}{\int (T_{1L} T_{2L} + T_{1R} T_{2R} + T_{1L} T_{2R} + T_{1R} T_{2L}) d\psi}.$$

Defining

$$\int A(\vec{a}, \lambda) B(\vec{b}, \lambda) \rho(\lambda) d\lambda = P_{\text{exp}}(\vec{a}, \vec{b}),$$

we can write

$$\begin{aligned} P_{\text{meas}}(\vec{a}, \vec{b}) &= \frac{N_{LL} + N_{RR} - N_{LR} - N_{RL}}{N_{LL} + N_{RR} + N_{LR} + N_{RL}} \\ &= P_1 P_2 P_{\text{exp}}(\vec{a}, \vec{b}) \\ &\quad + C_g [1 - |P_1 P_2 P_{\text{exp}}(\vec{a}, \vec{b})|^2] \cos(\vec{a}, \vec{b}). \end{aligned}$$

Measuring P_1 , P_2 , and C_g , the experimental counting rates can be used to extract $P_{\text{exp}}(\vec{a}, \vec{b})$.

Now we must remind the reader that in order to derive the inequality of Bell it is necessary to vary \vec{a} as well as \vec{b} (see Sec. II). Because in the laboratory system the two proton directions form

90° and not, as in the center-of-mass system, 180°, when rotating \vec{a} and \vec{b} around the propagation direction of the protons to \vec{a}' , \vec{b}' , the vectors \vec{a} , \vec{b} , \vec{a}' , and \vec{b}' are not coplanar. The prediction of QM is

$$P_{QM}(\vec{a}, \vec{b}) = C_{nn} \cos(\vec{a}, \vec{b}) + C_{np} \sin\varphi_1 \sin\varphi_2 \\ = C_{nn} \cos\varphi_1 \cos\varphi_2 + C_{np} \sin\varphi_1 \sin\varphi_2,$$

where φ_1 , φ_2 are the angles by which the analyzers are turned out of the reaction plane. Using this correlation function directly one sees that it does not violate the inequality of Bell. This comes from the fact that our analyzers are sensitive only to the transversal component of the polarization. Nonetheless, it is possible to obtain a contradiction using the fact that most of the scattering passes through a $J=0$ intermediate state and the correlation function of $J=0$ must be invariant with respect to rotation. We can decompose the correlation function into a part $f(\vec{a}, \vec{b}) = f(\varphi)$ that is rotationally invariant, and another part $g(\vec{a}, \vec{b})$ that is not, with

$$P(\vec{a}, \vec{b}) = f(\varphi) + g(\vec{a}, \vec{b}),$$

and therefore

$$P(\vec{a}, \vec{b}) - g(\vec{a}, \vec{b}) = P(\vec{a}', \vec{b}') - g(\vec{a}', \vec{b}')$$

if $(\vec{a}, \vec{b}) = (\vec{a}', \vec{b}')$. We define β such that $|g(\vec{a}, \vec{b})| \leq \beta$ for all \vec{a}, \vec{b} . The singlet scattering cannot contribute to the part of $P(\vec{a}, \vec{b})$ that is not rotationally invariant. Therefore an upper limit for β is the probability of triplet scattering. From the measurements of Catillon *et al.*¹⁹ one obtains

$\beta \leq 0.02 \pm 0.01$. We make the following assumption:

H4: An upper limit for the contribution of triplet scattering can be obtained from the scattering of polarized protons on polarized protons. This assumption could be eliminated by the use of a 90° (electrostatic) deflector before one of the polarimeters. This would give a 180° correlation and thus the vectors \vec{a} , \vec{b} , \vec{a}' , and \vec{b}' would be coplanar. Introducing the above expressions in the equality gives

$$|P(\varphi) + P(\varphi')| + |P(\varphi + \gamma) - P(\varphi' + \gamma)| \leq 2 + 4\beta \leq 2.08,$$

where φ , φ' and $\varphi + \gamma$, $\varphi' + \gamma$ are the angles that one polarimeter is turned out of the reaction plane, whereas the other remains fixed in the reaction plane.

Quantum mechanics predicts that

$$P_{exp}(\theta) = -C_{nn} \cos\theta,$$

when one analyzer is in the reaction plane and the other is rotated by an angle θ out of it (Fig. 2). Experimental values obtained by Catillon *et al.*¹⁹ can be interpolated to the energies used for this

experiment (13.2 and 13.7 MeV) and give $C_{nn} = -0.95 \pm 0.015$. The deviation of C_{nn} from -1 reflects the 2% contribution of triplet scattering. In order to get a contradiction between predictions of quantum mechanics and the inequality of Bell, we need some additional assumptions (H1 – H4).

Because the analyzing power and the transmission are similar to the experiment with annihilation γ 's, equivalent assumptions are needed. The main difference for protons is the fact their coherence length is $\sim 10^{-13}$ cm, which is extremely small compared to the dimension of the apparatus (~ 5 cm), whereas for the photons the coherence length is larger than or comparable to the size of the measuring apparatus. Therefore for photons the locality condition seems not as clear as in the present experiment.

Even if in the atomic cascade experiments it is possible to construct polarizers of nearly 100% analyzing power and transmission, the assumption made concerning the response probability of the photomultipliers is qualitatively the same as needed here, only it concerns a more simple effect (photoelectric effect) than the scattering process here, and is better isolated from other effects such as analyzing power.

B. Design of the experimental device

The design of the experimental device is mainly conditioned by the low transmission of polarization analyzers available in nuclear physics. For the analyzers used here it was of the order of 10^{-5} ; because of the coincidence between the analyzers only roughly one of 10^{10} pairs of protons which enter in the analyzers is detected in coincidence. To have, in spite of this, high enough counting rates, it is necessary to have a high beam intensity, thick targets, and large solid angles.

As hydrogen targets, polyethylene (CH_2) foils of 9 mg/cm² were used. The beam used of 1.5 μA with a spot size of 1.5-mm diameter instantly burned a hole in the target. Therefore it was necessary to construct a target rotating in an eccentric way with respect to the beam with the speed of 1 rev/sec. Thus, mechanically, the targets well withstood the beam, but still a chemical burning resulted in a blackening of the target and, after some hours, the hydrogen content on the beam trace diminished by a factor of 2. Thus every two hours the eccentricity was changed together with the orientations of the analyzers and every six hours the target was changed. Because the detectors were cooled to -20°C , ice buildup by the humidity contained in air had to be avoided and thus the opening was done under argon atmosphere.

The main problem for the analyzer was the reduction of the background. γ rays, mainly from the target, produce a background which rises exponentially for low energies and which completely covers the events of interest if one does not take great care. This background was reduced to essentially zero in the region of interest by a lead protection and by using silicon detectors 300 to 400 μ thick. The use of thinner detectors would have reduced the background even more but they would not have stopped the most energetic protons (~ 6 MeV) and thus the energy spectrum would have been deformed, not allowing a detailed interpretation. A careful design of slits is necessary to reduce the background produced by protons. The protons which are scattered by an angle $< 10^\circ$ leave the analyzer by a tube which serves at the same time as a rotation axis. The mean angle of scattering of the protons detected in the analyzer was fixed to 50° .

The final design of the analyzers is shown in Fig. 3. In an early stage of the experiment, one of the analyzers contained only two detectors. This was changed to have simultaneously a measurement of the geometric correlation (see Sec. IV F). All

pieces, including beam-defining slits, were mounted on the cover of the scattering chamber and aligned to better than $\frac{1}{10}$ mm. The most important dimensions are given in Table II.

C. Monte Carlo simulation

Apart from suitable experimental tests, it seemed highly desirable to make exact calculations simulating the experimental device in order to have a supplementary control that the apparatus not show any undesirable and uncontrolled feature. At the same time this provides help for the choice of geometry and for the optimization of the apparatus. A numerical integration is excluded because of the dimension of the integrals involved. Thus a Monte Carlo evaluation of the integrals was programmed for the CII 10020 computer.

The geometry was treated exactly taking into account the three dimensions of the device. The energy loss in the targets was calculated using the tables of Northcliff and Schilling.²⁰ Angular straggling was taken into account. The carbon cross section and polarization were obtained using the results of phase-shift analyses.²¹⁻²⁴ The

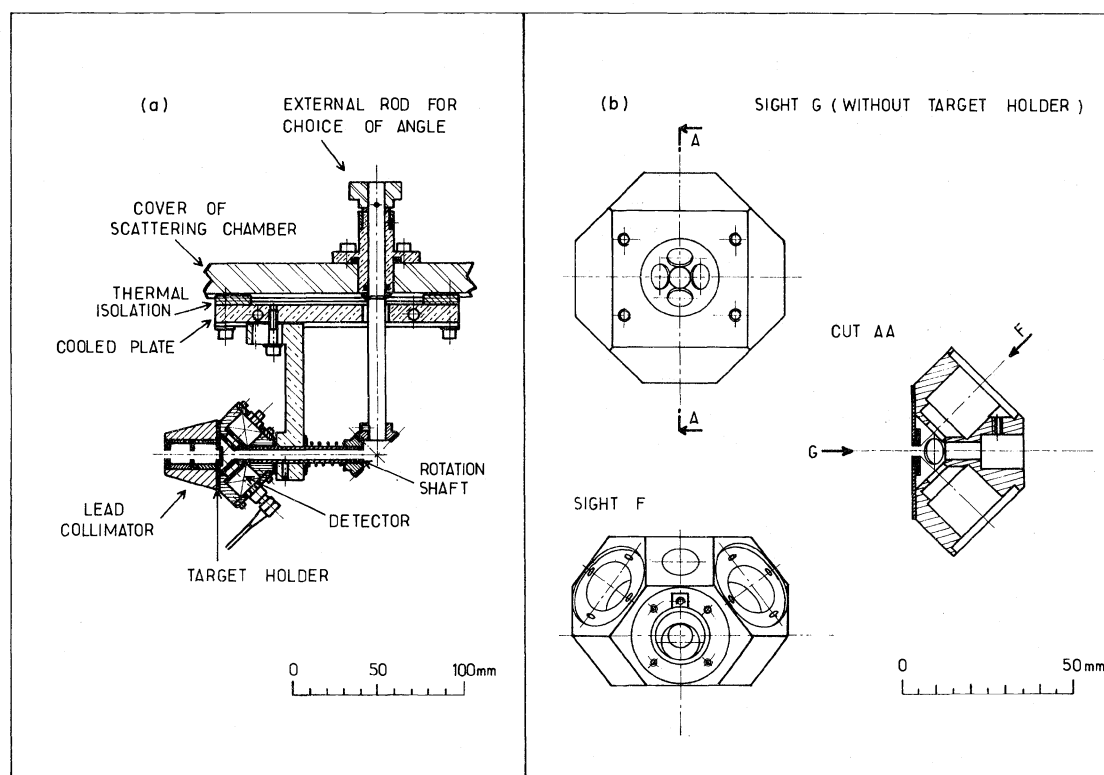


FIG. 3. Design of the polarization analyzers: Part (a) shows the general design, and part (b) shows the details of the analyzer.

TABLE II. Most important dimensions used in the experimental device.

	Diameter (mm)	Distance (mm) from target	Number
beam-defining slit 1	2	180	1
beam-defining slit 2	2	150	1
beam-defining slit 3	1.5	50	1
beam-defining slit 4	2	20	1
entrance slit of the analyzers	4.5	51.5	1
slit before detectors	7	12.5	2

phase shifts were parametrized and resonances at 4808 and 5373 keV (see Ref. 22) were included. Good agreement with published²¹⁻²⁴ cross sections and analyzing powers was obtained. For Ta scatterers pure Rutherford scattering was assumed, which is justified because the energy of the protons is much lower than the Coulomb barrier.

In the following the experimental results will be compared to the results of the Monte Carlo calculation.

D. Measurement of the analyzing power

The analyzing power was measured in a double-scattering arrangement. A beam of protons of 8.07 MeV is scattered by a 2-mg/cm² carbon target. The scattered protons enter at $\theta_{\text{lab}} = 70^\circ$ in the analyzer and are scattered with a mean angle of 50° a second time by the carbon foil of the analyzer, and one measures the asymmetry of the counting rates of the left-right detectors. Polyethylene foils are put between the first and second target to slow down the protons to the desired energy. The protons after the first scattering are polarized to 100% with an error of less than 2%.^{21, 22} Thus the analyzing power is directly obtained by the measured asymmetry. Before the measurement of the analyzing power the carbon target of the analyzer was replaced by a gold target (35 mg/cm²) to be sure that no misalignment affected the results.

The main problems connected with these measurements, once the background problem was solved, were target problems. First we used, for the analyzer, carbon targets prepared with Aquadag (Acheson Company). For proton energies above 6 MeV the experimental analyzing power was much lower than the calculated one, as stated in Ref. 25. Exposing the targets to the beam showed no significant target contamination. Heating them for several days to 200°C gave no improvement. But when these targets were heated in a vacuum to 1500°C they lost 20% of their weight, demonstrating that they contained still

a large amount of the liquid solvent. After heating to 1500°C the targets were so frail that they could no longer be used. Thus the targets finally used were mechanically worked out of solid carbon (Carbone Lorraine).

In Fig. 4 a typical energy spectrum is shown. The results of the asymmetry measurements for the two targets used, 18.6 and 29 mg/cm², are shown in Figs. 5 and 6. A background correction of about 2% was applied with an estimated error of 1%. The transmission of the analyzer, defined as the number of protons detected by the two detectors in the reaction plane divided by the number of protons which enter the analyzer, was 4.4×10^{-5} and 6.5×10^{-5} for the 18.6-mg/cm² and the 29-mg/cm² targets respectively.

E. Electronics associated with coincidence measurements

A block diagram of the coincidence measurements which will be described below is shown in Fig. 7.

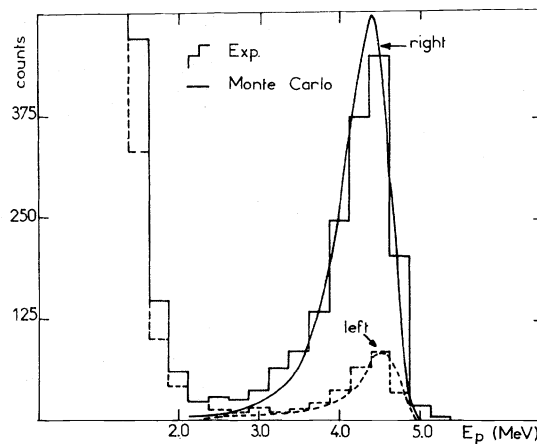


FIG. 4. Typical energy spectrum obtained in the measurement of the analyzing power of the polarimeters by double scattering of the protons, with $E_p = 8.07$ MeV, a first target of carbon of 2 mg/cm² and a second carbon target of 18.6 mg/cm². The protons entering in the analyzer were slowed down by a 17-mg/cm² CH₂ foil to $E_p = 5.95$ MeV.

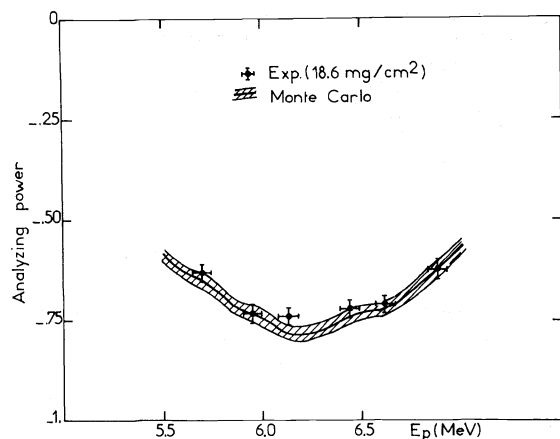


FIG. 5. Analyzing power of the analyzer with a 18.6-mg/cm² carbon target, as a function of the energy of the incoming protons. The width of the Monte Carlo calculation shows the uncertainty which was used to calculate the errors of the final results.

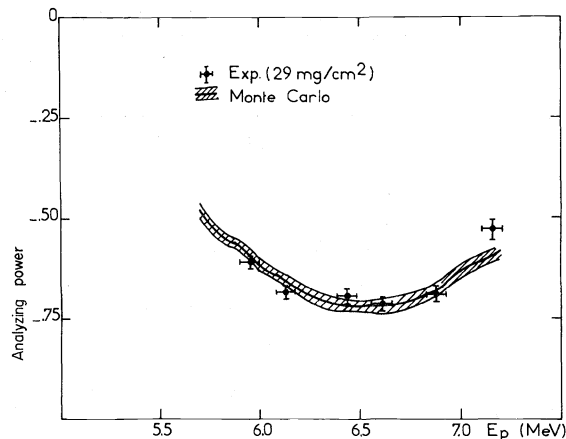


FIG. 6. Same as Fig. 5 for a 29-mg/cm² carbon target.

All the electronic devices up the analog-to-digital converters (ADC) used were standard electronics developed at the SPNBE at Saclay,²⁶ and they provide great versatility and facility toward a fast logic control of coincidence, anticoincidence, dead time, selection of energy domain, and con-

trol of counting rates at each level before the numerical analysis.

The four detectors of each analyzer are connected to a device which delivers a rapid pulse if one, and only one of the detector pulses delivered by a rapid proportional amplifier, is above a discriminator level. If there is a coincidence in the time-to-pulse converter, linear gates are opened which let the slower energy pulse of the

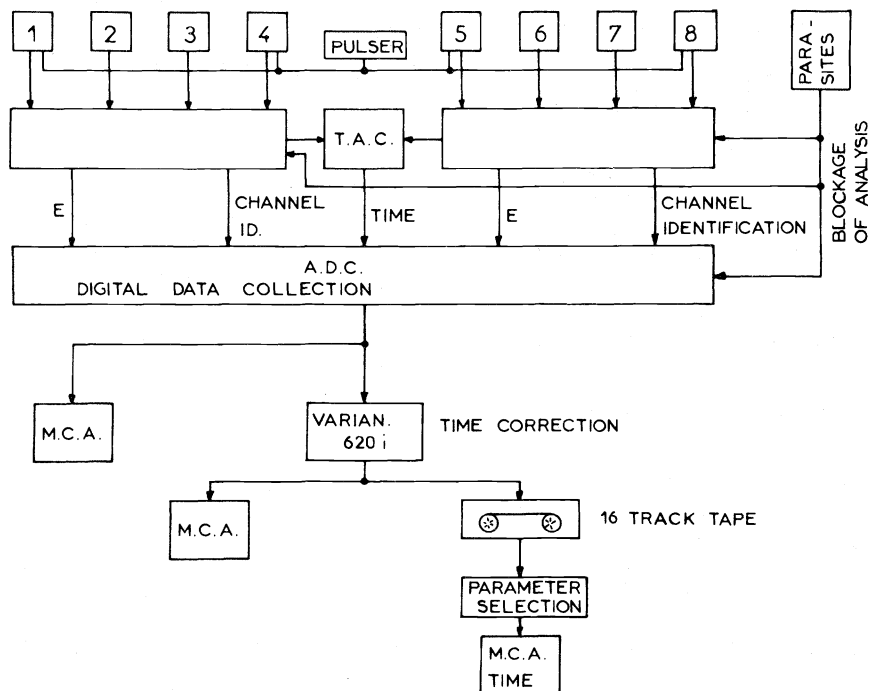


FIG. 7. Block diagram of the electronic setup used for coincidence measurements.

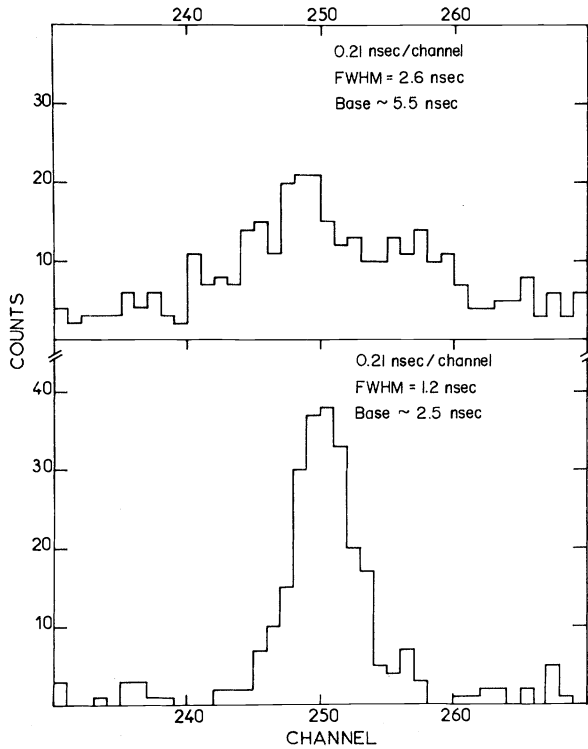


FIG. 8. Typical time spectra before and after rise-time correction by the 620 I Varian computer.

two, and only of these, detectors in coincidence pass, and an order is given to the ADC to analyze the energy and time signals. The results of this analysis together with an identification of the detectors in coincidence are sent to a Varian 620 I computer. This computer had mainly two roles: It coded the spectra following the 16 possibilities of coincidence and made a correction for the finite rise time (~ 50 nsec) of the rapid pulses. The rise-time correction was done by the formula

$$t_c = t_o + \frac{C_1}{E_1 + D_1} - \frac{C_2}{E_2 + D_2} ,$$

where t_o and t_c are the uncorrected and the corrected times, $E_{1,2}$ is the pulse height (energy) of the signals, and C, D were adjusted to give the best time resolution. A typical uncorrected and corrected time spectrum is shown in Fig. 8. A pulse generator was used continuously to control the electronic setup.

A good protection against electric parasites had to be included to prevent these parasites from simulating coincidences. A first protection is the anticoincidence between detectors which should not be in coincidence. A supplementary protection is given by an amplifying chain mounted in the same conditions as for the detectors. A discriminator is set just above the noise, and if it delivers a pulse, the coincidence circuits at the rapid level are blocked and the analysis of the pulses by the ADC is inhibited for 200 μ sec. With these safeguards it was verified that over a period of several days no parasites were analyzed.

The Varian 620 I computer delivers for each event sequences containing the two energies, the corrected time, and the coded coincidence possibility, together with the number of the run. This information is written on magnetic tape. After an appropriate energy selection the 16 time spectra are accumulated in a 4096-channel memory. Because the information was written event-by-event on magnetic tape, various controls could be made out of beam time. For example, it was verified, by repeating the data reduction with different energy windows, that the results were insensitive to the setting of the energy windows within reasonable limits.

F. The geometric correlation

The geometric correlation which arises from the kinematic correlation between the protons after the first scattering and the anisotropy of the carbon (p, p) cross section gives rise to an enhancement of the coincidences between left-left and right-right detectors with respect to the

TABLE III. Results of the measurements of the geometric correlation and comparison with Monte Carlo predictions (see text).

E_p (MeV)	Target (analyzer 1)	Target (analyzer 2)	C_g (Monte Carlo)	C_g (experiment)
13.7	Ta (70 mg/cm ²)	Ta (70 mg/cm ²)	0.26	0.22 \pm 0.01
	Ta (70 mg/cm ²)	C (27 mg/cm ²)	0.17	0.12 \pm 0.02
	C (27 mg/cm ²)	C (27 mg/cm ²)	0.11	0.07 \pm 0.02
13.2	Ta (70 mg/cm ²)	Ta (70 mg/cm ²)	0.26	0.225 \pm 0.01
	Ta (70 mg/cm ²)	C (18.6 mg/cm ²)	0.15	0.10 \pm 0.03
	C (18.6 mg/cm ²)	C (18.6 mg/cm ²)	0.09	0.05 \pm 0.02

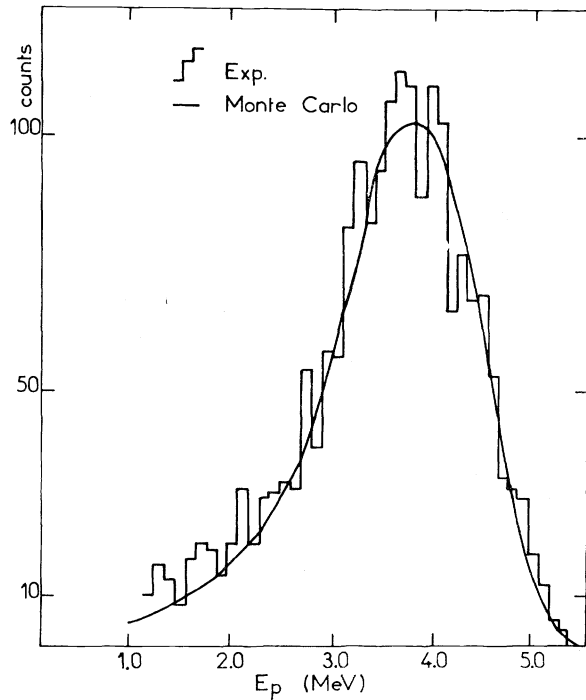


FIG. 9. Typical energy spectrum obtained in coincidence between the two analyzers with a 29-mg/cm² carbon target. Accidental coincidences have been subtracted.

right-left coincidences. Two methods were used to determine the coefficient of geometric correlation.

One method consists of first measuring the geometric correlation with both carbon foils in the analyzers replaced by 70-mg/cm² tantalum foils. The analyzing power of tantalum is zero; thus the measured correlation function is, for one pair of detectors in the reaction plane and the other rotated out of it by an angle θ , $P(\theta) = C_g(\text{Ta-Ta})\cos\theta$, where $C_g(\text{Ta-Ta})$ is the geometric correlation coefficient for this arrangement. At the same

TABLE IV. Final results for the measured correlation function $P_{\text{meas}}(\theta)$ as a function of the angle θ for 18.6-mg/cm² and 29-mg/cm² targets. Errors are statistical one-standard-deviation errors.

θ	18.6 mg/cm ²	29 mg/cm ²
0°	-0.40 ± 0.05	-0.38 ± 0.025
30°	-0.38 ± 0.04	-0.27 ± 0.025
45°	-0.29 ± 0.04	-0.26 ± 0.023
60°	-0.24 ± 0.04	-0.17 ± 0.025
90°	-0.01 ± 0.03	-0.03 ± 0.04

time this setup permits an easy control of the electronic setup and of the whole apparatus; the coincidence rates (about 1000 counts/hour and coincidence possibility) are about a factor of 100 larger than with the carbon foils. Then one replaces one tantalum foil by a carbon foil and one gets the coefficient $C_g(\text{Ta-C})$. The coefficient for two carbon foils is connected to these coefficients by the relation

$$C_g(\text{C-C}) = \frac{C_g(\text{C-Ta})^2}{C_g(\text{Ta-Ta})}.$$

The second method is provided by the measurement with two carbon foils, one pair of detectors turned out of the reaction plane by 90°, and the other by an angle θ . Then $P_{\text{exp}}(\theta) = 0$ (see Sec. III) and $P_{\text{meas}}(\theta) = -C_g\sin\theta$. Because the analyzers contained two detector pairs with 90° between them, simultaneously with the final results the value for the geometric correlations was obtained. Both methods gave within error bars identical results. The results are given in Table III.

As can be seen, the Monte Carlo simulation predicts a somewhat higher geometric correlation.

TABLE V. Final results for $P_{\text{exp}}(\theta)$ as compared to QM and to the limit of Bell. The results are given separately for the 18.6-mg/cm² and the 29-mg/cm² targets together with their weighted mean. $\langle P_1 P_2 \rangle$ and C_g are the values of the product of the analyzing power and of the geometric correlation coefficient, respectively, which were used to extract the values of P_{exp} from the values of P_{meas} given in Table IV.

θ	29 mg/cm ² $\langle P_1 P_2 \rangle = 0.44 \pm 0.025$ $C_g = +0.07 \pm 0.02$	18.6 mg/cm ² $\langle P_1 P_2 \rangle = 0.52 \pm 0.025$ $C_g = 0.05 \pm 0.02$	Mean	Bell's limit for the absolute value	QM
0°	-0.99 ± 0.09	-0.85 ± 0.11	-0.93 ± 0.07	≤ 1	-0.90
30°	-0.74 ± 0.08	-0.81 ± 0.10	-0.77 ± 0.06	≤ 0.69	-0.78
45°	-0.69 ± 0.08	-0.63 ± 0.09	-0.66 ± 0.06	≤ 0.52	-0.64
60°	-0.48 ± 0.07	-0.50 ± 0.10	-0.48 ± 0.06	≤ 0.38	-0.45
90°	$+0.07 \pm 0.10$	-0.01 ± 0.07	$+0.02 \pm 0.05$	≤ 0.02	0

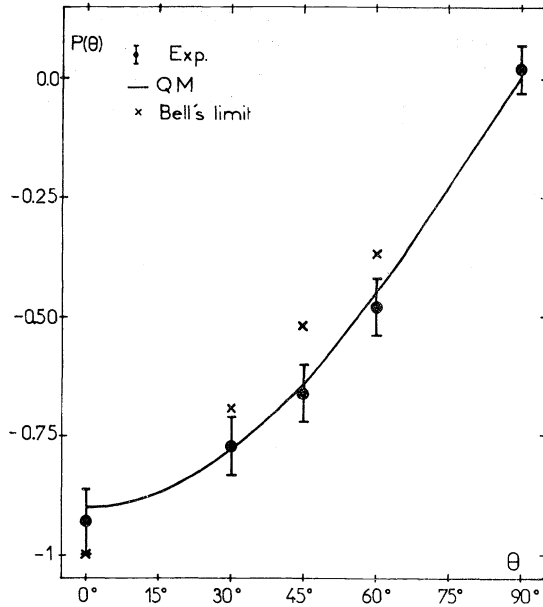


FIG. 10. Experimental results (see Table V) for $P_{\text{exp}}(\theta)$ as compared to the limit of Bell and predictions of QM.

The angular straggling mainly in the first target has some influence on the geometric correlation. To be sure that the values from Ref. 27 used in the Monte Carlo code were not the cause of this disagreement, we measured in a special device the angular straggling for the different targets; a good agreement was found.

The Monte Carlo calculation given in Table III was done for a perfect alignment of the apparatus. All misalignment contributes coherently to reduce the geometric correlation. Allowing for misalignment within the experimental uncertainties, $\frac{2}{10}$ mm for the center of gravity of the beam spot and $\frac{1}{10}$ mm for other geometric misalignments, the Monte Carlo code well reproduces the experimental results. These calculations showed, too, as one would expect, that the product of the analyzing powers, $\langle P_1 P_2 \rangle$, is independent of such small misalignments.

G. Final results

After all these preliminary measurements the final measurements of the coincidences of the two analyzers with carbon scatters could be made. It was verified that the final results for the correla-

tion function did not depend on the lower limits set on the energies of the detected protons. A typical energy spectrum is shown in Fig. 9. Accidental coincidences, which represent about 5% of the total, have been subtracted. For each angle about 30 individual measurements were made with different combinations of orientations of the analyzers. A total of 10^4 true coincidences were accumulated. The final results for $P_{\text{meas}}(\theta)$ are given in Table IV. In Table V the results for $P_{\text{exp}}(\theta)$ together with the values of the product of the analyzing power and of the geometric correlation used to extract the value of $P_{\text{exp}}(\theta)$ are given.

In Table V the weighted mean of these results for $P_{\text{exp}}(\theta)$ is also given and compared to predictions of QM and to the limit of Bell. The quoted experimental errors are one-standard-deviation errors containing statistical errors and uncertainties in the analyzing power and in the geometrical-correlations coefficient. In Fig. 10, the values of Table V are shown. As can be seen, the agreement with QM is good, whereas the results are in contradiction with the limit of Bell with a statistical significance of $\frac{7}{10000}$. Using the prediction of QM for $P_{\text{exp}}(\phi_1, \phi_2) = C_m \cos \phi_1 \cos \phi_2$ one obtains

$$C_m = -0.97 \pm 0.05$$

in good agreement with the value of $A_{yy} = C_m = -0.95 \pm 0.015$ of Catillon *et al.*¹⁹

V. CONCLUSION

The measurement of the spin correlation of protons gave good agreement with QM. To compare with the limit of Bell, as in previous experiments with photons, some extra assumptions are necessary. With these assumptions which seem natural but cannot be tested in our device, a contradiction is obtained with the limit of Bell providing an argument against the validity of this limit, and thus being in favor of nonlocal properties of microphysics.

All experiments performed up to now do not respect all the conditions necessary to permit a direct comparison with the limit of Bell. The conditions for transmission and/or analyzing power and the spacelike separation of the particles and the different parts of the measuring device²⁹ are not respected and seem very difficult to realize even extrapolating up today's techniques in spin or polarization correlation measurements. Thus it would be interesting to find some other type of experiments where it would be more easy to fulfill these conditions.

ACKNOWLEDGMENTS

We wish to thank J. S. Bell, B. d'Espagnat, and A. Shimony for helpful discussions. The support of this work by E. Cotton, C. Lévi, and L. Papin-

eau was appreciated. We thank the members of the mechanical workshop for very careful machining of all the pieces we needed and S. Valéro for the assistance and discussions during implantation of the Monte Carlo program.

*Present address: Univ. de Sao Paulo, Instituto de Fisica, C. Postal 20516, Sao Paulo, SP, Brasil.

¹A. Einstein, N. Podolsky, and B. Rosen, *Phys. Rev.* **47**, 777 (1935).

²E. Schrödinger, *Naturwiss.* **23**, 807 (1935).

³D. Bohm, *Phys. Rev.* **85**, 166 (1952); **85**, 180 (1952).

⁴J. S. Bell, *Rev. Mod. Phys.* **38**, 447 (1966); *Physics* (N.Y.) **1**, 195 (1964).

⁵A. Einstein, in *A. Einstein Philosopher Scientist*, edited by P. Schilpp (Library of Living Philosophers, Evanston, Ill., 1949).

⁶J. F. Clauser, M. A. Horne, A. Shimony, and R. Holt, *Phys. Rev. Lett.* **23**, 880 (1969).

⁷J. F. Clauser and M. A. Horne, *Phys. Rev. D* **10**, 526 (1974).

⁸J. S. Bell, in *Foundations of Quantum Mechanics*, proceedings of the International School of Physics, Varenna, 1970, "Enrico Fermi," Course 49, edited by B. D'Espagnat (Academic, New York, 1972).

⁹F. J. Belinfante, *A Survey of Hidden Variables Theories* (Pergamon, New York, 1973).

¹⁰D. Bohm, *Quantum Theory* (Constable, London, England, 1954).

¹¹L. R. Kasday, in *Foundations of Quantum Mechanics*, Ref. 8.

¹²S. J. Freedman and J. F. Clauser, *Phys. Rev. Lett.* **28**, 938 (1972).

¹³R. Fox, *Lett. Nuovo Cimento* **2**, 565 (1971).

¹⁴C. Faraci, D. Gutkowski, S. Notarrigo, and A. R. Pennisi, *Lett. Nuovo Cimento* **9**, 607 (1974).

¹⁵R. A. Holt and F. M. Pipkin, report (unpublished).

¹⁶N. F. Mott and F. E. Mayers, *Theory of Atomic Collisions*, 2nd ed. (Oxford Univ. Press, London, 1949).

¹⁷L. Wolfenstein, *Annu. Rev. Nucl. Sci.* **6**, 43 (1956).

¹⁸J. Raynal, *Nucl. Phys.* **28**, 220 (1961).

¹⁹P. Catillon, M. Chapellier, and D. Garreta, *Nucl. Phys. B2*, 93 (1967).

²⁰L. C. Northcliff and R. F. Schilling, *Nucl. Data Tables* **7**, 233 (1970).

²¹S. J. Moss and W. Haeberli, *Nucl. Phys.* **72**, 417 (1965).

²²C. W. Reich *et al.*, *Phys. Rev.* **104**, 143 (1956).

²³E. M. Bernstein and G. E. Terrel, *Phys. Rev.* **173**, 937 (1968).

²⁴J. S. Duval, A. C. L. Barnard, and J. B. Swint, *Nucl. Phys. A93*, 164 (1967).

²⁵G. Gurd, G. Roy, and H. Leighton, *Nucl. Instrum. Meth.* **61**, 72 (1968).

²⁶M. Avril *et al.*, *Compte rendu d'activité du Département de Physique Nucléaire*, Note No. CEA N-1232, 1968-1969 (unpublished), p. 66, and Note No. CEA N-1390, 1969-1970 (unpublished), p. 74.

²⁷J. B. Marion and F. C. Young, *Nuclear Reaction Analysis* (North-Holland, Amsterdam, 1968).

²⁸The experiment of Holt and Pipkin has been repeated very recently with a slightly different experimental device by J. F. Clauser [*Phys. Rev. Lett.* **36**, 1223 (1976)], and he obtained agreement with QM. E. S. Fry [*Phys. Rev. Lett.* **37**, 465 (1976)] made a measurement for another atomic cascade in Hg and obtained agreement with QM.

²⁹An experiment with atomic cascade is in progress at Orsay, Institut d'Optique, where the orientation of the polarizers will be changed randomly [A. Aspect, *Phys. Lett.* **54A**, 117 (1975)].